

Constraining dark energy evolution with gravitational lensing by large scale structures

Karim Benabed*

*Center for Cosmology and Particle Physics, Physics Department, New York University, New York, New York 10003, USA*Ludovic Van Waerbeke[†]*Institut d'Astrophysique de Paris, 98 bis Bd Arago, 75014 Paris, France*

(Received 26 June 2003; published 9 December 2004)

We study the sensitivity of weak lensing by large scale structures as a probe of the evolution of dark energy. We explore a two-parameters model of dark energy evolution, inspired by tracking quintessence models. To this end, we compute the likelihood of a few fiducial models with varying and nonvarying equation of states. For the different models, we investigate the dark energy parameter degeneracies with the mass power spectrum shape Γ , normalization σ_8 , and with the matter mean density Ω_M . We find that degeneracies are such that weak lensing turns out to be a good probe of dark energy evolution, even with limited knowledge on Γ , σ_8 , and Ω_M . This result is a strong motivation for performing large scale structure simulations beyond the simple constant dark energy models, in order to calibrate the nonlinear regime accurately. Such calibration could then be used for any large scale structure tests of dark energy evolution. Prospective for the Canada France Hawaii Telescope Legacy Survey and Super-Novae Acceleration Probe are given. These results complement nicely the cosmic microwave background and supernovae constraints.

DOI: 10.1103/PhysRevD.70.123515

PACS numbers: 98.80.Es, 98.62.Sb, 98.65.Dx

The need for dark energy in modern cosmology is driven by the necessity to describe the acceleration of the expansion of the Universe. Within this framework, the acceleration measured by the supernovae type Ia (SNIa) surveys [1,2] is explained by a new component added to the energy density of the Universe. In a Friedmann-Lemaitre-Robertson-Walker (FLRW) metric, this component is described by its equation of state (EOS), and the cosmological constant is one possible model, among others, of dark energy. Although the nature of dark energy remains unknown, different observations have been proposed to detect it, at least indirectly. Measurement of the supernovae distances [3–5] or the location of the cosmic microwave background (CMB) peaks [6,7] provide information on the modification of the distance/redshift relation by the dark energy. The evolution of large scale structures is also a probe of the dark energy: cluster abundances [8–10], Ly- α forest [11], strong [12,13] and weak lensing [14–18] are all sensitive to dark energy.

In this article, we investigate the weak lensing constraints on a varying equation of state. This case has been first investigated qualitatively by Benabed and Bernardeau [14] (hereafter BB01). Here, we expand their results to propose a new probe of a varying dark energy equation of state, based on the shear two-point function measured simultaneously in the nonlinear and linear regimes. The inclusion of the nonlinear structure formation process is particularly important, for the constraints on the dark energy using the linear regime alone are not particularly strong (which remains true even using the

tomography technique [16]). Here, we take into account the nonlinear regime of gravitational collapse, which is known to convey much of the dark energy sensitivity [14], to study the degeneracy of the dark energy parameters with the matter density Ω_M , the mass power spectrum shape Γ , and normalization σ_8 .

The sensitivity of the large scale structure growth to dark energy is due to the reduction of the gravitational collapse efficiency when the dark energy starts to dominate the energy budget of the Universe. The effect is a slower growth in the linear regime (for models within the current SNIa constraints). The more positive the first derivative of the pressure-over-density ratio w_D , the earlier this effect occurs and the more suppressed will be the structure growth. For a fixed amplitude of density fluctuations today, a slower growth means an earlier entrance of the fluctuations in the nonlinear regime, leading to more concentrated dark matter halos [19,20], and therefore “stronger” lenses [13]. As shown in BB01, the shear two-point function is sensitive to these two effects. It provides an unbiased measure of the projected density power spectrum in both the linear and nonlinear regimes, which is a direct test of the evolution of large scale structures, and consequently, of the evolution of dark energy. The transition scale between the linear and nonlinear scales is particularly a good tracer of the dark energy properties.

In the following, we first review the computation of the shear two-point function when a dark energy component is included. Then, we propose a simple two-parameter model that encompasses the major features of the very generic tracking quintessence models. Finally, we address the question of the efficiency of future lensing surveys to determine the dark energy properties.

*Electronic address: karim.benabed@physics.nyu.edu

[†]Electronic address: waerbeke@iap.fr

I. THEORY

This section is devoted to the theoretical basis for the results presented later in Sec. II. We give here a description of the nonlinear cosmic shear power spectrum with a nontrivial dark energy. We propose a suitable equation of state parametrization for the class of models studied here.

A. Background cosmology

Let us assume that the dark energy component interacts with the rest of the Universe via gravity only. The expansion of the Universe is completely described by the Friedmann equations

$$\left(\frac{\dot{a}}{a}\right)^2 = \frac{8\pi}{3M_{\text{Planck}}^2} \sum \rho_X \quad (1)$$

$$\frac{\ddot{a}}{a} = -\frac{4\pi}{3M_{\text{Planck}}^2} \sum (\rho_X + 3p_X), \quad (2)$$

and from an equation of state for each component

$$P_X = w_X \rho_X. \quad (3)$$

The radiation, matter and curvature equations of state are known. The only unknown quantity is the equation of state parameter of the dark energy, w_Q . It usually varies between $+1$ and -1 , the case $w_Q = -1$ corresponding to a cosmological constant. It has been proposed recently that w_Q could also take values lower than -1 [21]. When the dark energy component is assumed to behave like a scalar field, this is only possible if the field has a negative kinetic energy. However, such unusual behavior has only been found in very specific models [22], and we do not explore this possibility here. An equation of state with $w_Q > 1$ is also possible. It corresponds to a dark energy decreasing very quickly with time; for example, $w_Q = 1$ gives an evolution in a^{-6} . This kind of behavior is quite unlikely during the last stages of dark energy evolution, and will be indistinguishable from a standard Friedmann universe with no dark energy.

We assume that the dark energy does not clump; dark energy fluctuations are suppressed by the evolution, and clumping is only possible on the largest scales, near the horizon. Thus, the dark energy does not modify the primordial matter power spectrum in any other way than through modification of the expansion [6,23,24]. This modification only occurs when dark energy becomes subdominant, which translates into modification to the power spectrum at scales higher than the horizon size, much bigger than the ones probed by weak lensing.

With these assumptions, the impact of dark energy on the evolution of the large structures is completely described by the equation of state [25].

B. Shear measurements on distant galaxies

The deviation of light by the gravitational potential wells distorts the image of the distant galaxies. This shear effect can be used to probe the projected mass distribution along the line-of-sight (see [26] and references therein) from a measurement of the shape of the lensed galaxies. The lensing effect produced by the large scale structures is weak, but has already been measured (see [27,28] and references therein).

The gravitational lensing effect depends on the second order derivatives of the gravitational potential projected along the line-of-sight. The convergence κ and the shear γ describe, respectively, the isotropic and anisotropic distortions of the image of distant galaxies located at redshifts z_s . At linear order, convergence and shear field are related

$$\Delta\kappa = (\partial_1^2 - \partial_2^2)\gamma_1 + 2\partial_1\partial_2\gamma_2. \quad (4)$$

At the same order, the convergence in the direction θ for a galaxy at distance χ_s is given by:

$$\kappa(\theta) = \frac{3}{2} \frac{H_0^2}{c} \Omega_0 \int_0^{\chi_s} d\chi \frac{\mathcal{D}(\chi_s - \chi)\mathcal{D}(\chi)}{\mathcal{D}(\chi_s)} \frac{\delta[\mathcal{D}(\chi)\theta, \chi]}{a(\chi)}, \quad (5)$$

where $\chi_s(z_s)$ is the source radial distance at redshift z_s , and $a = 1/(1+z)$ is the scale factor. The radial distance at redshift z is given by

$$\chi(z) = \int_0^z dz' \frac{c}{H}. \quad (6)$$

The angular diameter distance \mathcal{D} is defined by

$$\mathcal{D}(\chi) = \begin{cases} \sin(\sqrt{K}\chi)/\sqrt{K}, & K > 1 \\ \chi, & K = 1 \\ \sinh(\sqrt{K}\chi)/\sqrt{K}, & K < 1, \end{cases} \quad (7)$$

where K is the curvature. The convergence power spectrum $P_\kappa(\ell)$ is a measurable quantity, and the equations above show that it is an unbiased estimate of the projected mass density contrast. It can be shown [29–31] (see [32] for notations) that it is directly related to the three-dimensional mass power spectrum P_{3D} via:

$$P_\kappa(\ell) = \frac{9}{4} \left(\frac{H_0}{c}\right)^4 \Omega_0^2 \int_0^{\chi_s} d\chi' \frac{g^2(\chi')}{\mathcal{D}^2(\chi')a^2(\chi')} P_{3D}\left(\frac{\ell}{\mathcal{D}(\chi')}, \chi'\right), \quad (8)$$

where the $g(\chi)$ function describes the lensing efficiency,

$$g(\chi) = \frac{\mathcal{D}(\chi_s - \chi)\mathcal{D}(\chi)}{\mathcal{D}(\chi_s)}. \quad (9)$$

For a broad redshift distribution $p_s(\chi)$ of the source galaxies, the observed signal is still given by Eq. (8),

but with a different efficiency function $g(\chi)$:

$$g(\chi) = \mathcal{D}(\chi) \int_{\chi}^{\chi_s} d\chi' p_s(\chi') \frac{\mathcal{D}(\chi_s - \chi')}{\mathcal{D}(\chi_s)}. \quad (10)$$

The source redshift distribution $p_s(z)$ is normalized, and usually parametrized as

$$p_s(z) = \Gamma^{-1} \left(\frac{1 + \alpha}{\beta} \right) \frac{\beta}{z_s} \left(\frac{z}{z_s} \right)^{\alpha} \exp \left[- \left(\frac{z}{z_s} \right)^{\beta} \right]. \quad (11)$$

The free parameters α , β , and z_s are adjusted to accommodate different lensing survey properties.

The ellipticity of the galaxies is an unbiased measure of the shear, from which we derive the convergence power spectrum (see the most recent reviews [27,28]). Various estimators can be used for this purpose, and the most practical one is the aperture mass variance as function of scale, $\langle M_{\text{ap}}^2(\theta) \rangle$ [33], because it provides a direct link between the observed shear and the projected mass density (which is of physical interest). Nevertheless, any two-point statistics could be used, and all we say about the aperture mass M_{ap} can easily be transposed to the top-hat variance and the shear correlation function. These statistics have already been measured on several lensing surveys [27]. The M_{ap} statistic at a scale θ_c is defined as the convergence smoothed with a compensated filter $U(\theta)$. Using Eq. (4), it is also given by a properly smoothed shear component γ_t :

$$M_{\text{ap}} = \int_0^{\theta_c} d^2\theta U(\theta) \kappa(\theta) \quad (12)$$

$$= \int_0^{\theta_c} d^2\theta Q(\theta) \gamma_t(\theta), \quad (13)$$

with $\int_0^{\theta_c} d\theta \theta U(\theta) = 0$, and where

$$Q(\theta) = \frac{2}{\theta_c^2} \int_0^{\theta_c} d\theta' \theta' U(\theta') - U(\theta). \quad (14)$$

The tangential shear γ_t at a location $\theta = (\theta \cos\varphi, \theta \sin\varphi)$ is defined by

$$\gamma_t(\theta) \equiv -\Re[\gamma(\theta) e^{-2i\varphi}]. \quad (15)$$

The choice of $U(\theta)$ is arbitrary provided it has a zero mean. In the following, we will use [27]

$$U(\theta) \equiv \frac{9}{\pi\theta_c^2} \left[1 - \left(\frac{\theta}{\theta_c} \right)^2 \right] \left[\frac{1}{3} - \left(\frac{\theta}{\theta_c} \right)^2 \right]. \quad (16)$$

For this particular choice, the variance of the convergence is expressed in terms of the shear power spectrum as

$$\langle M_{\text{ap}}^2 \rangle = \frac{288}{\pi} \int d\ell \ell P_{\kappa}(\ell) \left[\frac{J_4(\ell\theta_c)}{\ell^2\theta_c^2} \right]^2. \quad (17)$$

The variance of the aperture mass is a broadband estimate of the convergence power spectrum given in Eq. (8),

which can be directly estimated from the galaxy shapes. Predictions for the aperture mass require to compute the convergence power spectrum in dark energy models. A complete discussion on the computations of the weak lensing power spectrum with a cosmology with a non-trivial dark energy has been done in BB01. We only reproduce here the features of this work that will be used.

C. Cosmological distances

The relation between the cosmological distance and redshift is given by Eq. (6). The dark energy component leaves an imprint only on $\chi(z)$ by modifying the acceleration of the Universe obtained from Eqs. (1) and (2).

The modification of the distance-redshift relation affects mildly the convergence power spectrum. It can be summarized as the combination of two simple effects : a normalization change and a scale shift (similar to the modification of the position of peaks in CMB caused by the dark energy). In order to understand the mechanism, let us assume that the efficiency function [Eq. (9) and (10)], which has its maximum roughly at mid-distance between the observer and the source galaxies, can be replaced by a Dirac function

$$g^2(\chi) \sim g^2(\chi_{\text{mid}}) \delta(\chi - \chi_{\text{mid}}). \quad (18)$$

This galaxy selection can be approximated by replacing the $g(\chi)^2$ term in Eq. (8) by a Dirac function. Under this approximation, the normalization change is driven by the change in the position of the maximum of the selection function, and the scale shift comes from the $P_{3D}(\frac{\ell}{\mathcal{D}(\chi)})$ term in Eq. (8). The modification of the maximum of the efficiency window selects a different depth for projection.

In the following, we will show that the matter power spectrum can be split into two evolution regimes. At large scale, the linear regime is well described by a power law, and the effect of dark energy can be completely reabsorbed into a normalization change. At small scales however, in the nonlinear regime, the power law approximation breaks down, and the scale where the transition from linear to nonlinear regime takes place will be slightly shifted (this is also a similar effect in the CMB power spectrum).

D. Power spectrum of matter

We need to compute the power spectrum for a narrow range of scale, typically from a few arc seconds (galaxy scale) to a few hundred arc minutes across the sky. Large scales (> 5 degrees) are difficult to access observationally and are at the upper line of the largest surveys planned so far. At scales smaller than a few arc seconds (which is slightly smaller than a typical galaxy halo size), the number of lensed galaxies drops, and the noise blows up; no cosmological information can be extracted. At redshift one, a few degrees corresponds to a few hundred

Mpc, which is far below the horizon size at recombination. As stated in Sec. I A, we can safely assume that the cold dark matter model is a good description of the matter power spectrum. We have yet to investigate the evolution of the power spectrum from recombination until now with the presence of a dynamical dark energy component. At the linear order, it is given by the well-known equation [34]

$$\ddot{D}_+(t) + 2H\dot{D}_+(t) - \frac{3}{2}H^2\Omega_0(t)D_+(t) = 0. \quad (19)$$

In this equation, the matter acts as a source term which increases the depth of the potential well and tends to increase the density contrast. On the opposite, the expansion of the universe acts, via the second term, as a friction effect and reduces the efficiency of gravitation to increase the density contrast. This term carries all the effect of dark energy on the growth of structures. The well-known integral solution of Eq. (19) is valid when the universe only contains matter, radiation curvature, and a cosmological constant. It is also easy to check that there is no growing solution to Eq. (19) that can be integrated backward in time.

During the expansion, the growth follows the radiation, and later, the matter solution. When dark energy gets closer to the energy density of matter, the friction term grows compared to the source one. The efficiency of gravitational collapse to build up the density perturbation decreases and the growth of structures is damped. For the set of models where the dark energy happens to dominate earlier, this reduction of the growth rate is experienced at a higher redshift. The exact starting point of this damping depends on the evolution properties of the dark energy model. Models with $w_Q > -1$ experience this effect earlier than for $w_Q = -1$. For a constant equation of state, the energy density of the dark energy goes as

$$\Omega_Q \propto a^{-3(1+w_Q)}. \quad (20)$$

As said above, the $w_Q = -1$ model is the cosmological constant case. When $w_Q > -1$, Ω_Q grows when the scale factor a goes to unity. In this case, the dark energy contribution to the expansion is significant at a higher redshift than when $w_Q = -1$. This is even more important for varying w_Q , as shown Fig. 1. The modeling of the dark energy used in this figure will be described later.

Figure 2 shows the result of a numerical integration of Eq. (19) for different models. The damping of the growth appears earlier in the varying equation of state models, compared to the constant equation of state.

For a fixed redshift and for linear (i.e., large) scales, the modification of the structure growth is degenerate with the normalization of the power spectrum. A measurement of the power spectrum as a function of redshift would break this degeneracy. Unfortunately, the measured shear power spectrum is only a projection of the mass power

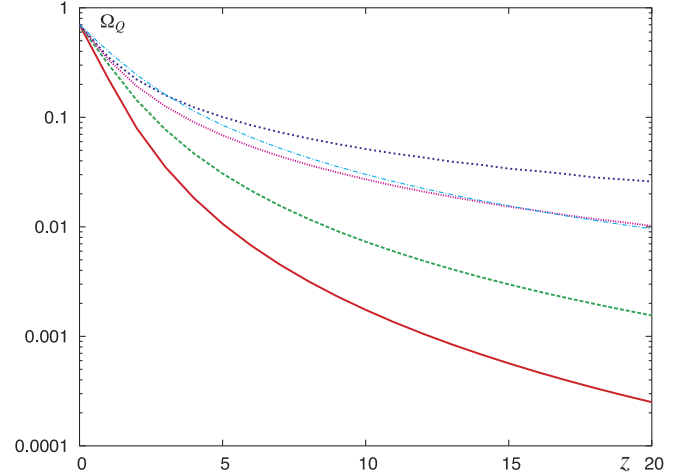


FIG. 1 (color online). The energy density of dark energy normalized to the critical density as a function of redshift. The solid line is the classic Λ model. The thick, long-dashed line and thin, dot-dashed line are, respectively, $w_Q = -0.8$ and $w_Q = -0.6$ models. The short-dashed line and dotted line are, respectively, $w_0 = -0.8, w_1 = 0.2$ and $w_0 = -0.8, w_1 = 0.3$ models (complete description of the parametrization can be found Sec. I E). The sooner the dark energy gets close to 1, the sooner it will affect the expansion and the growth of structure. As expected, models with an equation of state different from $w_Q = -1$ contribute significantly to the acceleration sooner. Models with a varying equation of state contribute yet sooner. A constant $w_Q = -0.6$ model interpolates between the two $w_1 \neq 0$ ones.

spectrum along the line-of-sight, and the integrated growth effect will be, in the linear regime, indistinguishable from a normalization shift.

At small scales, the evolution of the density contrast changes dramatically. Virialized objects are formed and evolve in a different regime than the simple one described by the linear approximation. BB01 showed that this regime could potentially break part of the degeneracy seen in the linear regime. The perturbation approach cannot describe this regime, for the density contrast is very high at the scale of virialized objects. A complete computation of this regime cannot be done analytically. One has to rely on numerical simulations to calibrate the nonlinear regime in a “generic” way. Several “classical” descriptions have been proposed (among others see [35–37]). We will follow here the choices made in BB01, namely, that the stable clustering ansatz provides a valid description of the smallest scales. It states that virialized objects are stable, that is to say that their physical size does not vary with the expansion of the universe. Hence, at the scale of these objects, the density contrast has to grow in order to match exactly the expansion. Instead of a growth of order a or smaller, the density contrast evolves as $a^{3/2}$. One should note that the scales described by the ansatz are much below the shear measurement scales. The transition between the linear and nonlinear regimes is described by a

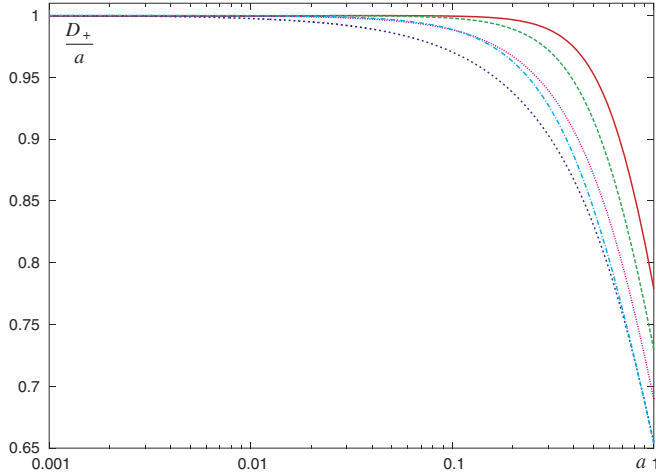


FIG. 2 (color online). Linear growth for different models. Models are the same as in Fig. 1. The growth is normalized to the recombination era. The modification of the equation of state induces a precocious acceleration that decreases the efficiency of gravitational collapse at higher redshift than in the $w_Q = -1$ case. A variation in the equation of state ($w_1 \neq 0$) amplifies this effect. As expected from Fig. 1, a constant equation of state model can partly mimic a varying equation of state: if one knows the CMB normalization and today normalization of the fluctuation of structures, one cannot distinguish between a $w_Q = -0.6$ and a $w_0 = -0.8$, $w_1 = 0.3$ model.

mapping between the two regimes [35], which is calibrated from N -body simulations, as described by Peacock and Dodds [36]. At large scale, the mapping keeps unchanged the linear regime, and at small scales, it goes as $(a^2/g^2P)^{3/2}$.

We should note that, even if it has been widely tested for many different cosmologies, this mapping has never been directly tested for dark energy models. Nevertheless, this is not an issue here. Indeed, numerical simulations will be performed in the future to further refine our knowledge of the nonlinear regime, even for “exotic” cosmological models. Already, the most recent progress on the subject [37] suggests an accuracy of 3–5% in the nonlinear regime prediction. This is to be compared to the effect of dark energy on the amplitude of the power spectrum which is found here to be around 10–20% for the models studied in Sec. II.

The assumption that N -body simulation can accurately describe the nonlinear clustering with quintessence is quite a strong assumption regarding the physical properties of the dark matter. It can partly be justified by the fact that it is unlikely that a smoothed dark energy component with no coupling will affect directly the small scale behavior of the matter. Its influence should only appear as a change in the expansion and thus, as we have shown, as a modification of the linear growth of structures. The strength of this argument is enhanced by a recent result from another description of the nonlinear regime usually

called the *halo model*. This approach describes the virialized object as dark matter halos of known¹ profile and abundance depending on the cosmological parameters [37]. The results and concepts behind this approach have been successfully tested in the context of dark energy [19,20]. In particular, the differences observed between halos in Λ cosmologies and in cosmology with nontrivial dark energy can be explained by an earlier entrance into the nonlinear regime. The observed discrepancies are, as expected, all explained by the modification of the linear growth of structures [14,17].

The fact that the structures will enter the nonlinear regime earlier will show up in the weak lensing power spectrum in two ways. First, because of the projection, the transition between the linear and nonlinear regimes occurs at smaller ℓ . Second, the increase of the amplitude of the power spectrum will be stronger at small scale than at large scale. BB01 proposed estimations of these two effects. In particular, due to the different evolution in the nonlinear regime, the modification of the asymptote height is expected to go as the third power of the normalization modification in the linear regime. At this point of the discussion, we would like to emphasize that any modification of the nature of the dark matter will likely be degenerate with the effect of dark energy (in terms of structure growth). For instance, a small hot dark matter component will also modify the growth rate. It is expected that this modification should decrease the amount of small scale structure, thus suppressing the effect of dark energy. We are then likely to underestimate the effect of dark energy in those models.

E. Dark energy model

The evolution of w_Q has to be fixed by a proper model of dark energy. Several models have been studied. The simplest one is the so-called *minimal quintessence model*, where w_Q is constant, and another interesting set of models is *tracking potential models*.

These models have been extensively described [38]. Their interest lie in the fact that w_Q is constant during most of the universe evolution, and that the constant equation of state is an attractor solution for w_Q when the expansion of the universe is dominated by another component (like the radiation or the matter). When the dark energy reaches the order of magnitude of the other energy densities, it leaves its attractor evolution. This attractor ensures that the initial conditions of dark energy do not have to be fine-tuned. For any starting value of the dark energy,² it has to reach the attractor and will always exit the domination of matter at the same point, which in turn depends on the exact model. This explains the inter-

¹Read *fitted on N-body simulations*.

²Usually the initial conditions are free within a few tens of order of magnitude.

est these models have met among the high energy physics community. In particular, it has been shown that some tracking potential models can be built within particle physics models. For example, P. Brax and J. Martin [39] proposed a version of the Ratra-Peebles model [40] that can be embedded in supergravity models.

Minimal and tracking models are not the only dark energy models available. The problem is that a common framework does not exist to describe the different dark energy models, that would allow a direct comparison with cosmological observations like weak lensing. To make such comparison possible, one has to parametrize the evolution of dark energy that can leave an imprint on the weak lensing power spectrum. As a consequence, we only have to consider its impact on the growth of structure and on the relation distance-redshift. We choose to parametrize the evolution of dark energy in terms of its equation of state. This choice is the most prevalent one. This is by no means the only possible parametrization (see, for example, [41,42]). As stated in Sec. IA, the knowledge of the EOS of dark energy is sufficient to solve Eqs. (1) and (2) and to compute $\chi(z)$ and D_+ .

As we described in Sec. IA, we assume that w_Q can freely vary between -1 and 1 . An easy solution is to decompose w_Q in terms of a power series of the redshift

$$w_Q = \sum w_i z^i. \quad (21)$$

The possible determination of the two first orders of this development has been studied in many different articles [3–5,43–47]. This is the way most SNIa data are analyzed, assuming the perturbative development

$$w_Q = w_0 + w_1 z \dots \quad (22)$$

This approach is not valid in our case: one can only compute the growth of structure from recombination, therefore a perturbative development as Eq. (22) is not suitable for our purpose for it leads to an unphysical, arbitrarily growing equation of state. Attempts have been made to generically describe dark energy with a simpler parametrization than the naive power series but they are not suitable for our purpose here. Some of them have too many parameters and are too general [48,49]. Others [50] do not share the same Taylor expansion as those models they are attempting to fit which is a feature we want to include in our modelization.

In order to reduce the complexity of the parametrization issue, we will only be interested in models which exhibit a behavior similar to the tracking potential models. There are few arguments in favor of these models. The behavior of the dark energy equation of state at large redshift is irrelevant for us. Indeed, tracking models ensure that the equation of state of the dark energy is constant as long as it is dominated by the other components [38]. In that case, a variation of w_Q has little or no

impact on the expansion of the universe, and the growth of structure is not affected. If one assumes that dark energy can be dominant at high redshift, this discussion is not valid. However, such a model would leave a huge imprint on the CMB and would be most probably already ruled out by observations.

At low redshift, when dark energy reaches the order of magnitude of the energy density of matter, it will start to contribute to the expansion, and induce a new period of acceleration. Variations of w_Q will leave a strong imprint on the shear power spectrum through modifications of the cosmological distances and structure growth. This is where our assumption on the shape of the EOS is important. It has been shown [51] that the equation of state of tracking models can be fitted at low redshift by a log function

$$w_Q \sim w_0 + w_1 \log(1 + z), \quad (23)$$

where w_0 and w_1 are free parameters. This behavior is roughly valid up to redshift $z \sim 1$ at least for SUGRA and Ratra-Peebles potentials. Note that this EOS admits Eq. (22) as Taylor expansion for small z . The parametrization given in Eq. (23) fails quickly above $z \sim 1$ (see Fig. 3); we used an arc tangent for higher redshifts:

$$w_Q = \begin{cases} w_0 + w_1 \log(1 + z), & \text{if } z \leq 1 \\ w_0 + w_1 [\log(2) - \arctan(1) + \arctan(z)], & \text{if } z > 1, \end{cases} \quad (24)$$

The arbitrary behavior at high z , which is $w_0 + w_1 [\log(2) - \arctan(1) + \pi/2]$, has no reason to fit the high z asymptote of a given tracking potential model. This is irrelevant for us as long as the energy density is dominated by the matter density. In the end, the only thing that matters is the evolution of dark energy from the epoch when it starts to dominate. This epoch can be at redshift as high as ten. For example, in a SUGRA $\alpha = 6$ model [39] the energy density of dark energy represents 10% of the total energy density at redshift as low as $z \sim 5$ (see Figs. 3 and 1).

The parametrization, Eq. (24), is not very good at fitting the equation of state. In Fig. 3, for instance, the fit agrees reasonably well with the SUGRA $\alpha = 6$ model. However, for our purpose, the relevant comparison is not for the EOS, but it is for the growth and distances of the different models, which are the quantities intervening into the power spectrum calculation (see Fig. 4).

The fit accuracy for the tracking models we tested is around 3%. Another advantage of this parametrization is that it is described by two parameters only, w_0 and w_1 . We have fixed the change between the log and tan branches to $z_c = 1$. This choice is arbitrary, and a small change in the value of z_c means a small modification of the growth of structure. A value $z_c = 1.5$ corresponds to 1% change in D_+/a , comparable with the error on the modeling. Overall, this arbitrariness on z_c leads to negligible mod-

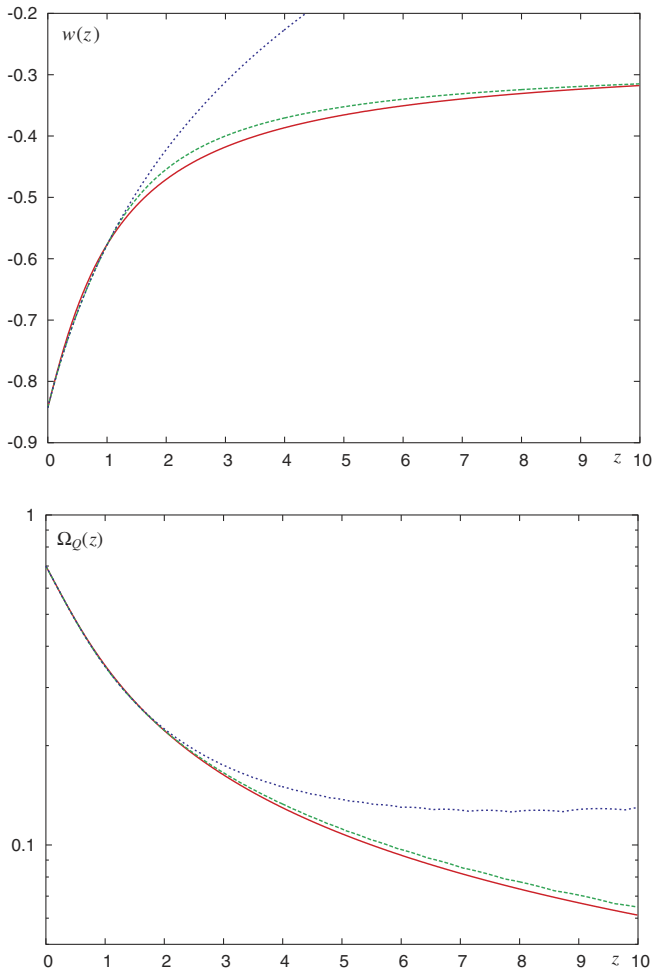


FIG. 3 (color online). Comparison between an explicit SUGRA model and its parametrization. The equations of state are presented in the top panel, whereas the energy density, normalized to the critical density are in the bottom panel. The solid line is the SUGRA $\alpha = 6$ model, the long-dashed line is the logtan parametrization [see Eqs. (23) and (24)]. The parameters $w_0 = -0.84$, $w_1 = 0.32$ are measured on the SUGRA model. The log parametrization quickly fails to fit the equation of state above $z \sim 1$. It keeps a relatively good agreement on the dark energy density to a higher redshift. It is not unexpected as the dominant contribution to H^2 is already the matter energy density. Thus slight variations on the equation of state of the dark energy are softened on Ω_Q . The discrepancy, however, builds up very quickly to a factor 2 around $z \sim 8$. While not being in perfect agreement with the SUGRA model, the logtan parametrization does a better job at following Ω_Q .

ifications in the cosmological distances and projection effect.³ Finally, since the parametrization (24) admits Eq. (22) as its Taylor expansion, our results are directly comparable with the well-known SNIa ones [5].

³We do have a small dependency on redshift higher than one through the broad distribution of the source $p_s(z)$. This effect is small enough to be neglected here.

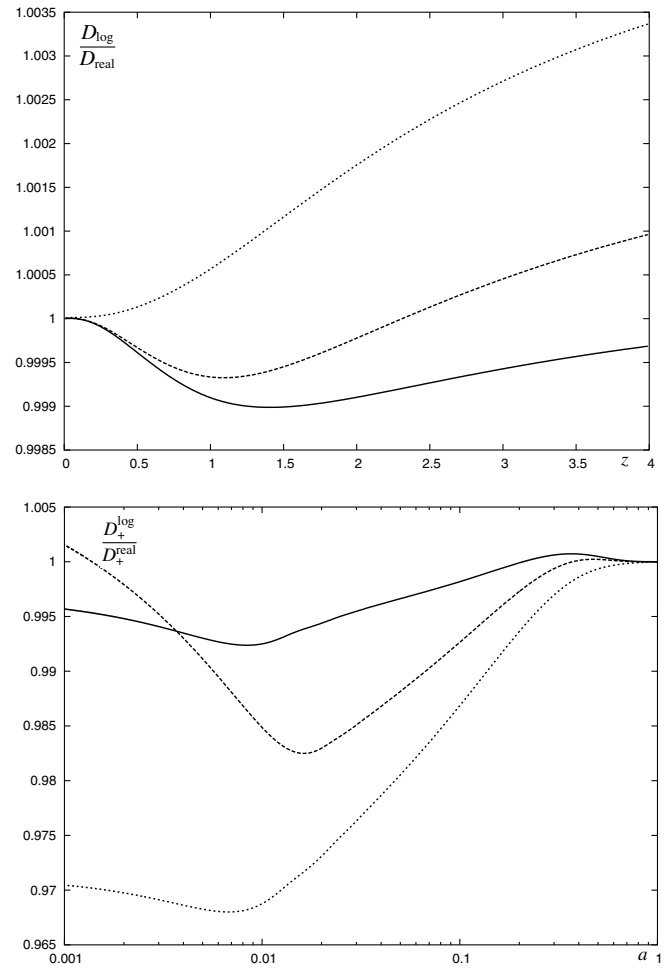


FIG. 4. Comparison between real tracking models and their approximated version using Eq. (24). The top panel presents the comoving distances, the bottom panel the growth of structure. The solid line is a SUGRA $\alpha = 6$ model, the dashed line a SUGRA $\alpha = 11$ model, and the dotted line a Ratra-Peebles, $\alpha = 4$ model. The discrepancy on the angular distances computed with the real model and our parametrization is below the percent up to $z = 4$. The discrepancy for the linear growth is of order 3% up to the recombination. Our approximated formula with its very small number of parameters gives a good approximation of the quantities on which are computed the weak lensing effect.

II. RESULTS

We perform a maximum likelihood analysis of the aperture mass statistic for a set of dark energy models. The method is well known and has been formerly described in [52]. Section II A describes the models and surveys that will be investigated. The numerical results are shown and discussed in Sec. II B.

A. Parameter estimation

We know from previous studies that the gravitational lensing by large scale structures depends mainly on four

TABLE I. Lensing surveys that will be part of the CFHTLS and SNAP projects (see text). Entries are source mean redshift \bar{z}_s , survey total area θ_{deg}^2 , source galaxy number density (per arcmin²), and intrinsic ellipticity dispersion σ_e .

	\bar{z}_s	θ_{deg}^2	n_{gal}	σ_e
CFHTLS	0.9	1790	20	0.44
SNAP	1.2	300	100	0.32

parameters: the matter energy density Ω_0 , the mass power spectrum normalization σ_8 , its slope, and the redshift of the sources [53]. As described above, we can safely ignore modification to the cold dark matter transfer function [54] due to dark energy. We thus use it and describe the slope of the power spectrum by the parameter Γ , which is supposed to include the subtle effects of baryons, neutrinos, any component that could potentially affect the power spectrum shape. There are specific sensitivities of the lensing effect on these parameters taken individually, but this is weak, and the complete study of all degeneracy directions is left for future work. We assume that the redshift distribution of the sources is known, because forthcoming optical surveys are expected to provide an accurate measurement of it from photometric redshifts. The redshift dependence is very similar to the σ_8 dependence, hence any uncertainty could be reabsorbed in a broader σ_8 prior, or constraint. Our set of free parameters is chosen as $\mathbf{p} = (w_0, w_1, \Omega_0, \sigma_8, \Gamma)$. We choose a flat universe prior, given that the current CMB results are in very good agreement with a flat geometry [55].

We compute the likelihood $\mathcal{L}(\mathbf{p}|\mathbf{d})$, where the data vector \mathbf{d} is the aperture mass $\langle M_{\text{ap}}^2 \rangle$ as function of scale:

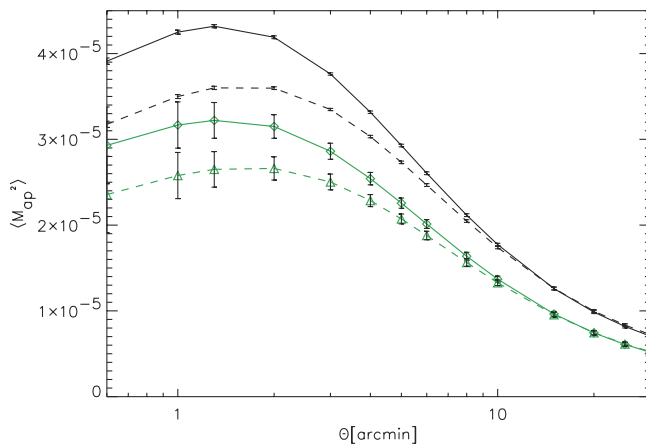


FIG. 5 (color online). Aperture mass variance as function of scale for model 3 (solid lines) and model 2 (dashed lines), for CFHTLS (thick bottom lines) and SNAP (thin top lines). The error bars show the statistical and sampling errors, assuming a Gaussian statistic for the sampling error.

$$\mathcal{L} = \frac{1}{(2\pi)^{n/2} |\mathbf{S}|^{1/2}} \exp\left[-\frac{1}{2}(\mathbf{d} - \mathbf{s})^T \mathbf{S}^{-1}(\mathbf{d} - \mathbf{s})\right], \quad (25)$$

where \mathbf{s} is the fiducial model vector and

$$\mathbf{S} \equiv \langle (\mathbf{d} - \mathbf{s})^T (\mathbf{d} - \mathbf{s}) \rangle \quad (26)$$

is the covariance matrix. The covariance matrix is computed following the method described in [53] assuming the Gaussian field approximation. In this work we are exploring two options: a large ground-based survey (such as the Canada France Hawaii Telescope Legacy

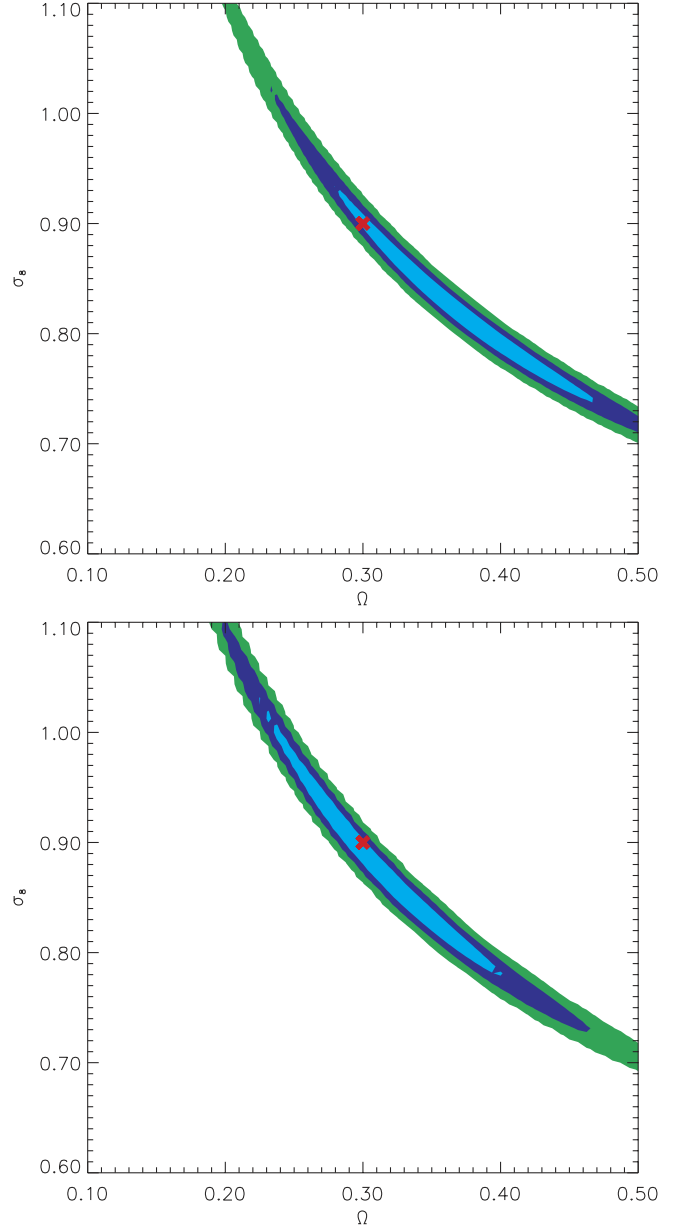


FIG. 6 (color online). Contours in the Ω_0 , σ_8 space when marginalized over the quintessence $w_0 \in [-1, -0.7]$ and $w_1 \in [0, 0.4]$. This is given for the CFHTLS experiment. The top panel corresponds to model 1, the bottom panel to model 2.

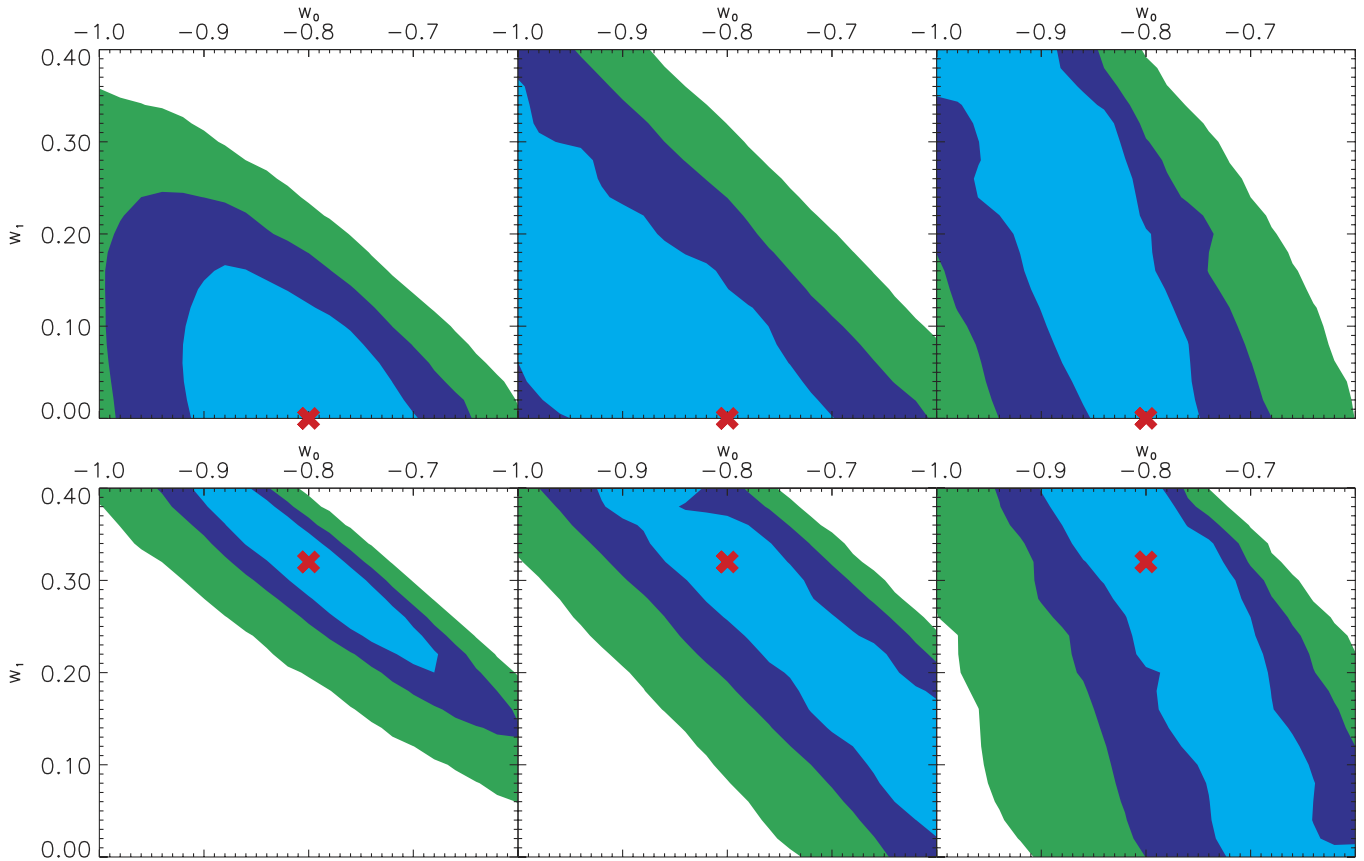


FIG. 7 (color online). CFHTLS constraints with lensing alone on w_0 and w_1 . Top panels: model 2, bottom panels: model 3. The left plots assume all other parameters are known (see Figs. 10 and 11). For the middle plots the mean density and the power normalization are marginalized (flat prior) over $\Omega_0 \in [0.1, 0.5]$ and $\sigma_8 \in [0.6, 1.1]$. The right plots show the contour for the marginalization $\Gamma \in [0.1, 0.4]$.

Survey (CFHTLS) [56]).⁴ and a space survey (such as the Super-Novae Acceleration Probe (SNAP) [57]).⁵ The observational properties of the lensing survey associated with these two projects are summarized in Table I.

For the two surveys, we selected three fiducial models (with a cosmological constant $\Omega_\Lambda = 0.7$):

- (i) model 1: $p_1 = (-1, 0, 0.3, 0.9, 0.24)$
- (ii) model 2: $p_2 = (-0.8, 0, 0.3, 0.9, 0.24)$
- (iii) model 3: $p_3 = (-0.8, 0.32, 0.3, 0.9, 0.24)$

The first model is a pure cosmological constant case. Second is a minimal dark energy model with no variation of the equation of state. This type of model is widely used in the literature. From the discussion of Sec. ID, it is expected that this kind of model undervalues greatly the effect of a varying EOS with identical final value. The last model has a varying EOS. The value of w_1 has been chosen in order to agree with an $\alpha = 6$ SUGRA model. It corresponds to a strongly evolving equation of state model. Models with a smaller w_1 interpolate between model 2 and model 3.

We also have to make a choice on the range of parameters we want to investigate. Maximum likelihood analysis with five parameters is already a computationally expensive task. It can be reduced in part by narrowing the range of the parameters and the number of points in each direction.

For the CFHTLS-like analysis, it is expected that we will mildly constrain the parameters. We thus used a relatively sparse grid and relatively wide parameter ranges. The matter density Ω_0 will be allowed to vary between 0.1 and 0.5, while σ_8 will be free between 0.6 and 1.1. The choices for these two parameters are quite conservative. They allow to probe the full one-sigma contour. The slope of the power spectrum is weakly constrained by the weak lensing measurement; we probe its values between 0.08 and 0.4. The results below (Figs. 9–11) show that the parameter space is correctly sampled.

For SNAP-like analysis, we greatly reduce the range of parameters. The precision required here forces us to increase the number of computed models, in particular, in the Ω_0, σ_8 space. We thus suppose that it is enough to probe Ω_0 between 0.28 and 0.32, and σ_8 between 0.85 and 0.95. Nevertheless, it is expected that by the time SNAP

⁴<http://www.cfht.Hawaii.edu/Science/CFHLS/>

⁵<http://snap.lbl.gov/>

will collect data, previous weak lensing measurements, CMB, galaxy and cluster surveys will have cut down the accuracy on these parameters below these levels. We conservatively keep a relatively wide range on Γ (0.1 to 0.3, in agreement with the results for CFHTLS).

For both models, we probed the dark energy parameter space between -1 and -0.6 for w_0 and 0 and 0.4 for w_1 . Note that we do not take into account models with an equation of state more negative than -1 , as we mentioned in the introduction. The upper bound on w_0 corresponds roughly to the degeneracy expected between our target varying equation of state and a constant equation of state model (see Sec. ID). We do not investigate negative w_1 models. Negative w_1 models are very close to the cosmological constant case, and should be strongly degenerated with it, with little hope for the observer to see anything. The w_1 upper bound corresponds to a strongly varying equation of state. The SUGRA and Ratra-Peebles models lie in between.

B. Numerical results—discussion

We first compute the aperture mass for our dark energy models. Figure 5 presents the results for SNAP and the CFHTLS surveys. It shows that the evolution of the dark

energy can lead to a 10 to 20% effect at small scale. As emphasized in Sec. ID, this is precisely the expected effect. This is a large effect, already accessible with the current data quality and measurement techniques, if all other parameters were known, with no systematics.

Next we perform the likelihood analysis on our target models. Figs. 9–11 show, respectively, the parameter predictions for the models 1, 2, and 3. All possible combinations of pairs of parameters are plotted in order to show the direction of degeneracies. On each plot, the two hidden parameters are assumed to be perfectly known. We first note the strong degeneracy between the dark energy parameters (w_0, w_1) and the other parameters. The full degeneracy between w_1 and Γ is understood by the fact that the shape parameter describes the slope of the power spectrum, for a fixed normalization σ_8 . Changing Γ will modify the ratio between linear and nonlinear regime and the scale of transition. As shown in Sec. ID, a change in w_1 has a similar effect.

Even allowing for dark energy, the shear two-point function remains a good constraint on Ω_0 and σ_8 . Figure 6 shows the effect of unknown dark energy parameters (marginalized on w_0 and w_1) on the measurement of Ω_0 and σ_8 . For the pure cosmological constant

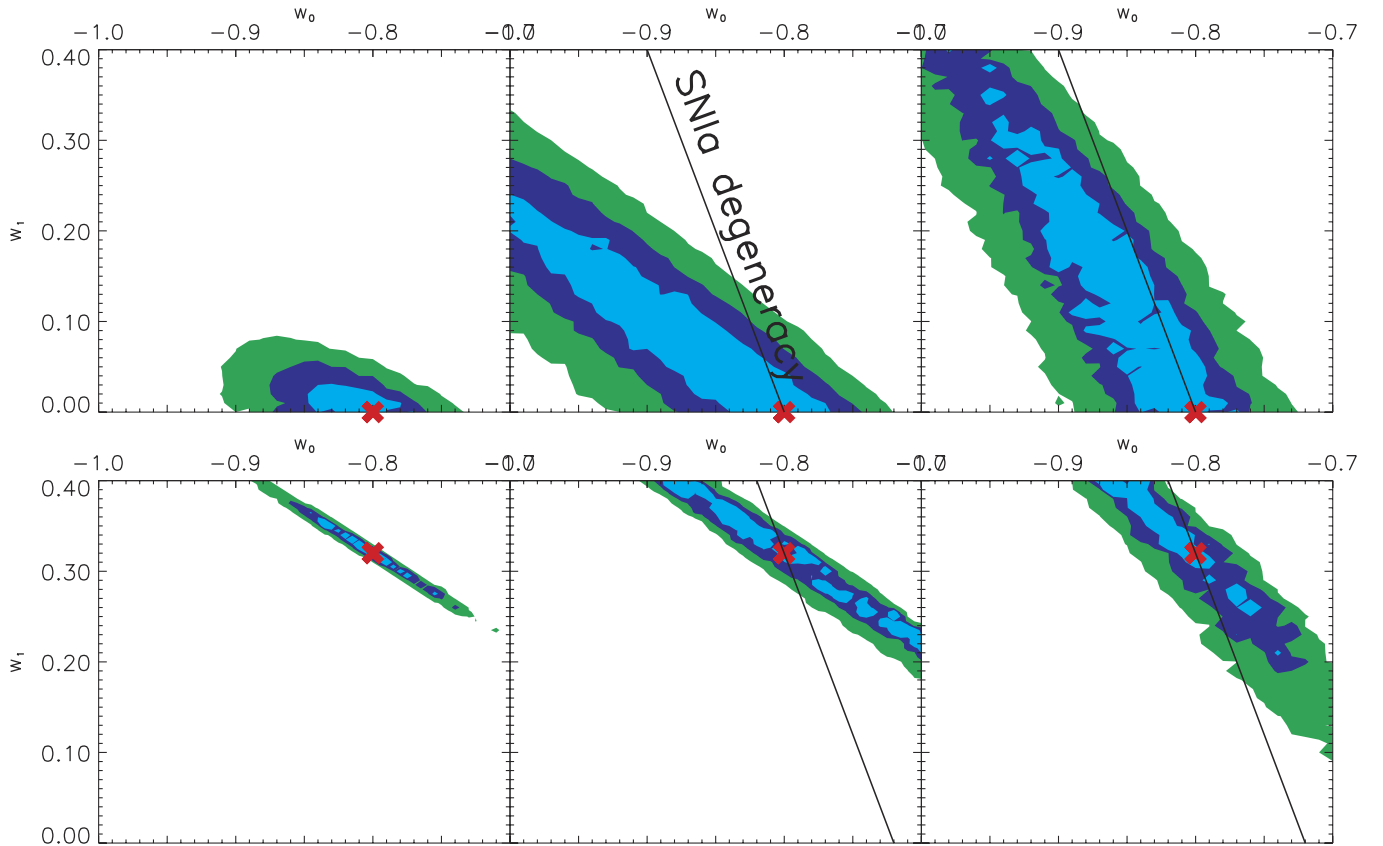


FIG. 8 (color online). Same as Fig. 7 for the SNAP survey. The marginalization is performed over the intervals $\Omega_0 \in [0.28, 0.32]$ and $\sigma_8 \in [0.85, 0.95]$ for the middle plots and $\Gamma \in [0.1, 0.3]$ for the right plots. The lines show the direction of degeneracy of the SNIa (with the supposition of a perfect Ω_0 knowledge).

model (top panel), we see that the most probable models correspond to higher Ω_0 and lower σ_8 than the fiducial model. For the model 2 (bottom panel), the normalization is underestimated. This figure shows that the widths of the Ω_0 , σ_8 contours are not dramatically affected, but the most probable models are changed.

Supernovae surveys have a small sensitivity to the variation of the equation of state. In particular, it is expected that without a strong prior on Ω_0 they cannot provide much information on w_1 [3–5,43–47]. The question is whether the shear two-point function also suffers from this kind of limitation or not. Figures 7 and 8 show the predictions for w_0 and w_1 , respectively, for the CFHTLS and SNAP cosmic shear predictions. The left panels correspond to the contours obtained with a perfect knowledge of Ω_0 , σ_8 , and Γ . The middle panels are for a known Γ , but marginalized over Ω_0 and σ_8 . The right panels are for known Ω_0 and σ_8 , and marginalized over

Γ . The top panels are for model 2, and the bottom panels for model 3. The important result here is that the marginalization over Ω_M and σ_8 do not increase too much the widths of the contours; it only restores a degeneracy between w_0 and w_1 .

Contrary to the angular diameter distance tests, the weak lensing is sensitive to the evolution parameter w_1 . The marginalization over Γ restores the degeneracy along a different direction, but still does not increase the contours' widths significantly. It means that even with a limited knowledge on external important parameters, it is still possible to constrain the quintessence, in particular, when it evolves with time. In that case indeed (i.e., $w_1 \neq 0$), the increase of the lensing signal is large enough to allow the CFHTLS observations to rule out a pure cosmological constant case. However, an accurate joint measurement of the quintessence parameters and the others is not possible using the lensing power spectrum

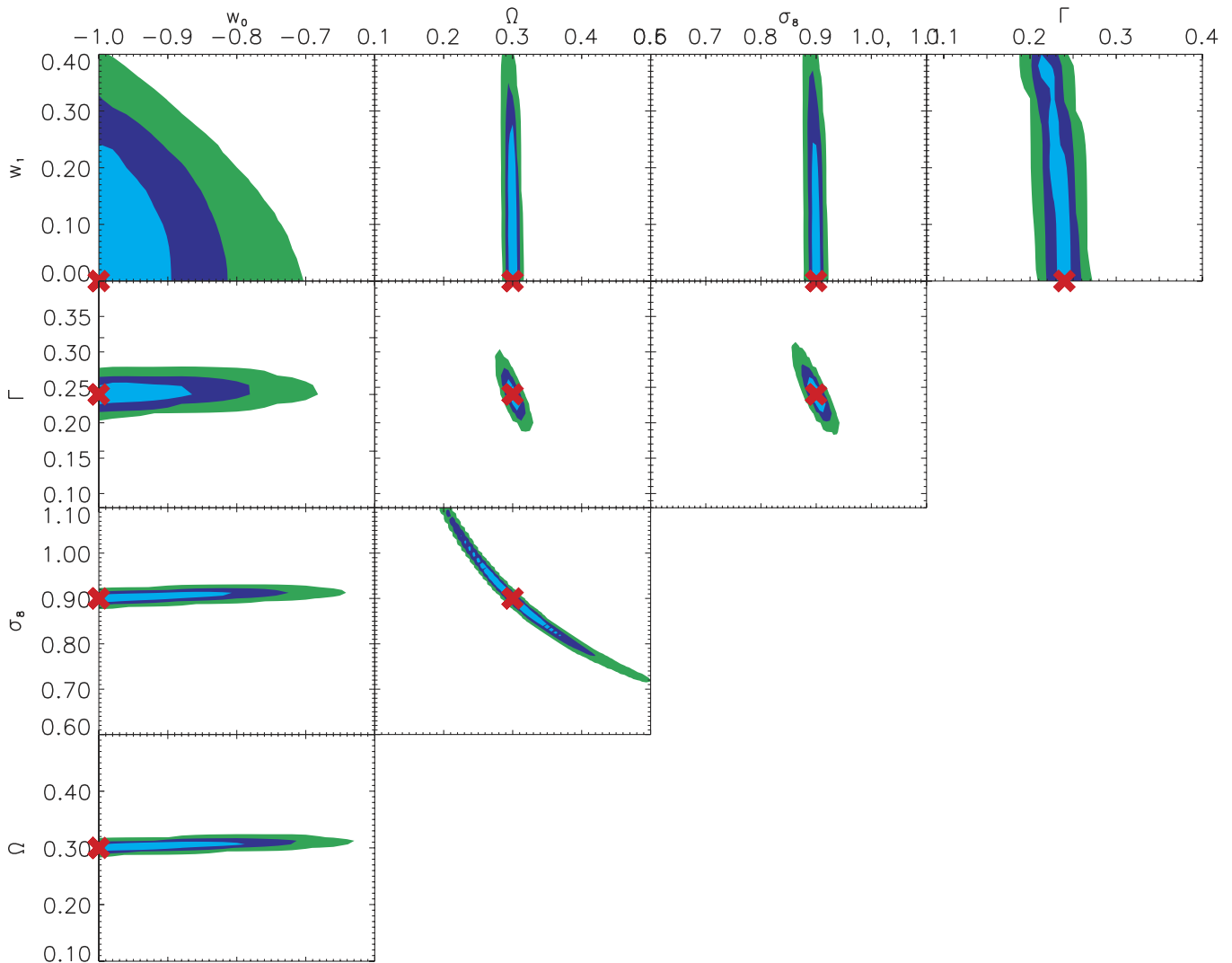


FIG. 9 (color online). Constraints obtained with the CFHTLS survey for a cosmological constant model (model 1). We assumed strong prior for the hidden (not shown) parameter on each plot. The cross represents the fiducial model.

alone, because of the strong degeneracy between Ω_0 and σ_8 .

This degeneracy is broken with the SNAP lensing survey: according to Fig. 8, one sees that cosmic shear observations alone with the SNAP satellite, provide constraints which are competitive with the SNIa constraints from the same satellite. The expected constraints from SNIa alone, assuming a perfect knowledge of Ω_0 , is sketched on this figure (solid line). It shows that SNIa are less sensitive to w_1 than weak lensing. Therefore a combination of SNIa and cosmic shear could simultaneously probe the dark energy and its evolution. More precisely, Figs. 9–11 show that the knowledge of w_0 is irrelevant for constraining Ω_0 from cosmic shear. On the other hand, the SNIa measurements are degenerate between w_0 and Ω_0 . A combination of the two experiments provide a simultaneous measure of w_0 and Ω_0 without the need for an external measurement of Ω_0 . We can then use the lensing constraints on w_0 and w_1 (Figs. 7 and 8) to

estimate the dark energy evolution w_1 . In fact even a poor knowledge of Ω_0 could be tolerated; we know from [5,44,45] that a marginalization over Ω_0 of the SNIa measurements increases the w_0, w_1 contours perpendicular to the increase of the same contours from cosmic shear with poor knowledge on Ω_0 (Figs. 7 and 8, middle panels). Adding the cosmic microwave background overconstrains the parameter space, because the contours in the Ω_0, w_0 space are “perpendicular” to the SNIa and cosmic shear constraints [55]. Weak lensing, cosmic microwave background, and SNIa provide therefore an ideal set of complementary experiments for constraining the dark energy beyond the constant energy density case [58], because weak lensing measurement breaks the degeneracy with the dark energy evolution.

Earlier work has shown that cosmic shear provides also independent constraints on Ω_0 from the measurement of high order statistics of the convergence [59–62]. Dark energy modifies mildly this picture. At the level of the

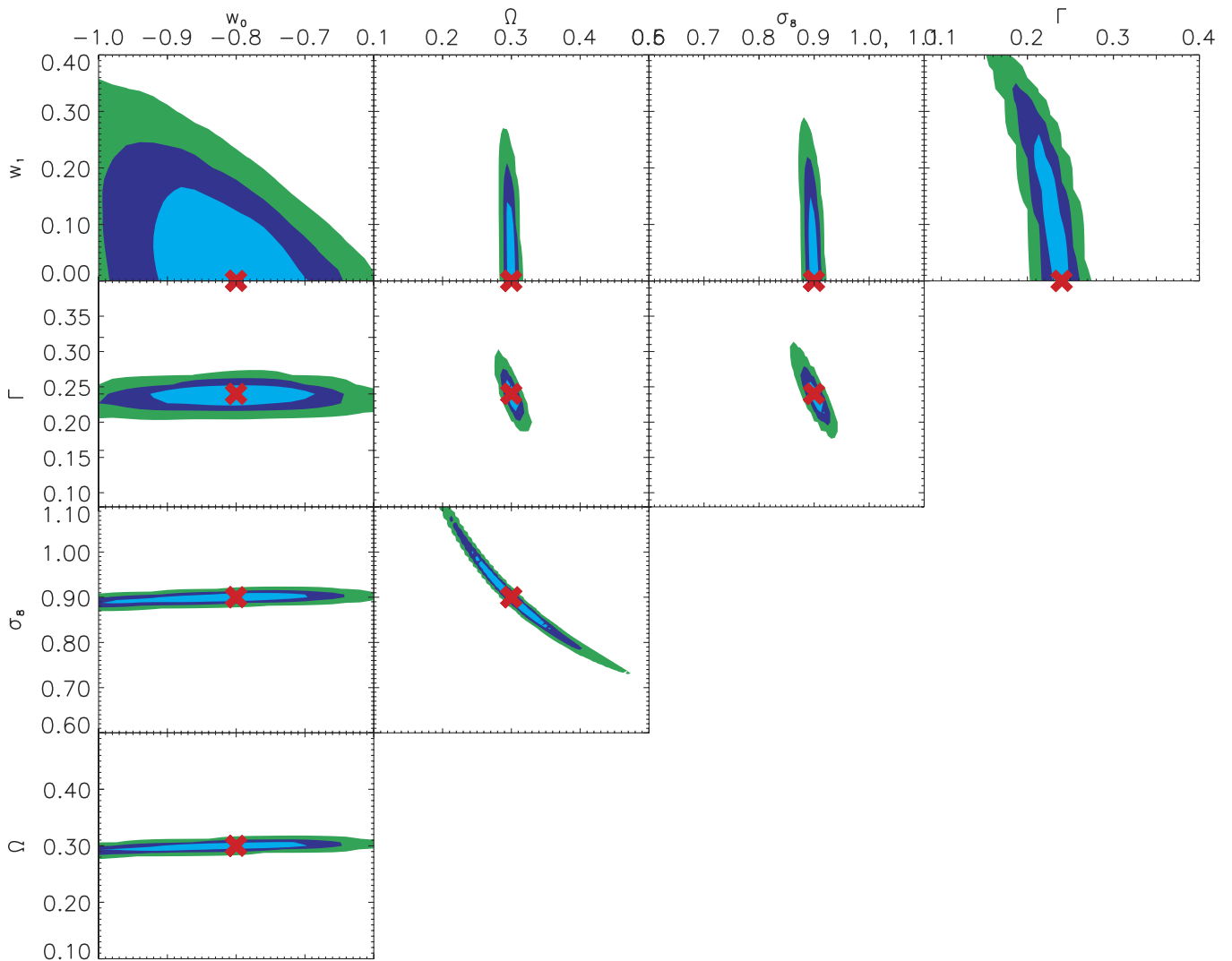


FIG. 10 (color online). Same as Fig. 9 for a quintessence, nonevolving model 2 (see Table I).

quasilinear regime, it only affects the three-point function of the convergence field through the projection effect [14]. The modifications are expected to be more important at small scales [63]. One can see from Figs. 9–11 that this additional information is not necessary, given the degeneracy among w_0 in the (w_0, Ω_0) space. However, such external constraint could be very helpful to pin down the degeneracy with σ_8 , and consequently to reduce the degeneracy between w_0 and w_1 , helping to narrow the constraint on w_1 .

III. CONCLUSION

We investigated the possibility to constrain the evolution of dark energy evolution from measurements of the gravitational lensing by large scale structures. We used the fact that the nonlinear growth rate of structures is significantly affected. This is a consequence of an earlier influence of dark energy on the expansion of the Universe.

It was found that the cosmic shear effect is a good probe of the evolution of dark energy, in opposition with experiments based on angular diameter distances only, like SNIa and cosmic microwave background, which are better suited to measure the “constant” part w_0 of dark energy equation of state (in a particular parametrization). The degeneracy with other parameters (Ω_0 , σ_8 , and Γ) restores a degeneracy between w_0 and w_1 , but the widths of the contours in that space are slightly affected. Therefore a linear combination of w_0 and w_1 is well measured using weak lensing, even with a poor knowledge on Ω_0 and σ_8 .

It is generally believed that the measurement of the dark energy equation of state parameter as a constant is such a difficult task that we should not even dream to measure its evolution. We have shown here, for a class of models, that the sensitivity of the large scale structures to a simple evolution parameter w_1 is as easy (or difficult!) as w_0 to measure. Consequently, we found out that a

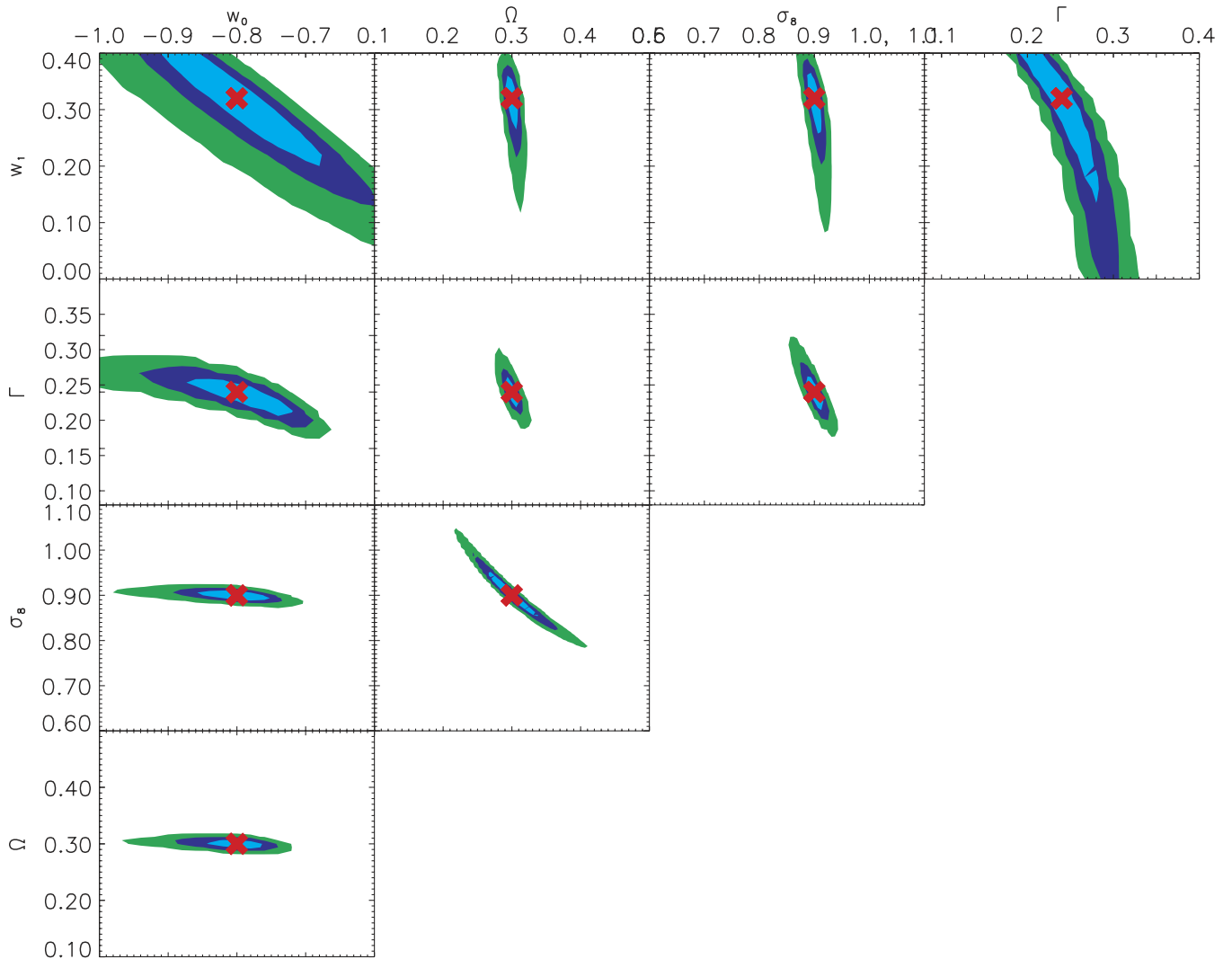


FIG. 11 (color online). Same as Fig. 10 for an evolving dark energy model (model 3).

combination of cosmic shear, SNIa, and cosmic microwave background provide orthogonal constraints of the parameters w_0 , w_1 , and Ω_0 , which opens great opportunities to probe nontrivial models of dark energy. For the set of models studied here, we found that these three experiments overconstrain these parameters.

One should note that the difference in the amplitude of the cosmic shear signal between model 2 ($w_0 = -0.8$, $w_1 = 0$) and model 3 ($w_0 = -0.8$, $w_1 = 0.32$), at scales below $5'$, reaches 10%. This is large compared to the statistical errors of the CFHTLS and SNAP surveys. However, it is yet within the limits of the point spread function (PSF) correction and nonlinear modeling accuracies [52]. If one wants to measure the dark energy evolution as proposed here, it is clear that we need to perform ray-tracing simulations for the class of models we want to investigate, in order to calibrate the nonlinear modeling [64]. The PSF correction is an entirely different

issue, which is not discussed here, but there is good hope to be able to reduce the systematics level by a factor of 5 to 10 [65], which should be enough for our purpose here.

Redshift degeneracy was not discussed, but it is not different from the σ_8 and the Ω_0 degeneracies. What has been said for these parameters also applies to the source redshift. In the future, photometric redshifts will provide accurate source redshift measurements, as we do not need an accurate redshift for each lensed galaxy.

ACKNOWLEDGMENTS

The authors acknowledge useful discussions with F. Bernardeau, O. Doré, B. Fort, M. Joyce, Y. Mellier, D. Pogosyan, R. Scoccimarro, and J-P. Uzan. K. B.'s research is supported by NSF Grant No. PHY-0101738. The likelihood computations were run on the NYU Beowulf cluster supported by NSF Grant No. PHY-0116590.

-
- [1] S. Perlmutter, G. Aldering, G. Goldhaber, R. A. Knop, P. Nugent, P. G. Castro, S. Deustua, S. Fabbro, A. Goobar, D. E. Groom *et al.*, *Astrophys. J.* **517**, 565 (1999).
 - [2] A. G. Riess, P. E. Nugent, R. L. Gilliland, B. P. Schmidt, J. Tonry, M. Dickinson, R. I. Thompson, T. Budavári, S. Casertano, A. S. Evans *et al.*, *Astrophys. J.* **560**, 49 (2001).
 - [3] P. Astier, *Phys. Lett. B* **500**, 8 (2001).
 - [4] I. Maor, R. Brustein, and P. J. Steinhardt, *Phys. Rev. Lett.* **86**, 6 (2001).
 - [5] M. Goliath, R. Amanullah, P. Astier, A. Goobar, and R. Pain, *Astron. Astrophys.* **380**, 6 (2001).
 - [6] P. Brax, J. Martin, and A. Riazuelo, *Phys. Rev. D* **62**, 103505 (2000).
 - [7] M. Doran and M. Lilley, *Mon. Not. R. Astron. Soc.* **330**, 965 (2002).
 - [8] Z. Haiman, J. J. Mohr, and G. P. Holder, *Astrophys. J.* **553**, 545 (2001).
 - [9] J. Weller, R. A. Battye, and R. Kneissl, *Phys. Rev. Lett.* **88**, 231301 (2002).
 - [10] W. Hu, *Phys. Rev. D* **67**, 81304 (2003).
 - [11] U. Seljak, R. Mandelbaum, and P. McDonald, *astro-ph/0212343*.
 - [12] M. Bartelmann, M. Meneghetti, F. Perrotta, C. Baccigalupi, and L. Moscardini, *Astron. Astrophys.* **409**, 449 (2003).
 - [13] M. Sereno, *Astron. Astrophys.* **393**, 757 (2002).
 - [14] K. Benabed and F. Bernardeau, *Phys. Rev. D* **64**, 83501 (2001).
 - [15] D. Huterer, *Phys. Rev. D* **65**, 63001 (2002).
 - [16] W. Hu, *Phys. Rev. D* **66**, 83515 (2002).
 - [17] M. Bartelmann, F. Perrotta, and C. Baccigalupi, *Astron. Astrophys.* **396**, 21 (2002).
 - [18] N. N. Weinberg and M. Kamionkowski, *Mon. Not. R. Astron. Soc.* **341**, 251 (2003).
 - [19] A. Klypin, A. V. Maccio', R. Mainini, and S. A. Bonometto, *Astrophys. J.* **599**, 31 (2003).
 - [20] E. V. Linder and A. Jenkins, *Mon. Not. R. Astron. Soc.* **346**, 573 (2003).
 - [21] S. M. Carroll, M. Hoffman, and M. Trodden, *Phys. Rev. D* **68**, 023509 (2003).
 - [22] V. K. Onemli and R. P. Woodard, *Classical Quantum Gravity* **19**, 4607 (2002).
 - [23] P. G. Ferreira and M. Joyce, *Phys. Rev. D* **58**, 23503 (1998).
 - [24] M. Malquarti and A. R. Liddle, *Phys. Rev. D* **66**, 123506 (2002).
 - [25] M. S. Turner and M. White, *Phys. Rev. D* **56**, 4439 (1997).
 - [26] M. Bartelmann and P. Schneider, *Phys. Rep.* **340**, 291 (2001).
 - [27] L. Van Waerbeke and Y. Mellier, *astro-ph/0305089*.
 - [28] A. Refregier, *Annu. Rev. Astron. Astrophys.* **41**, 645 (2003).
 - [29] J. Miralda-Escude, *Astrophys. J.* **380**, 1 (1991).
 - [30] N. Kaiser, *Astrophys. J.* **388**, 272 (1992).
 - [31] F. Bernardeau, L. van Waerbeke, and Y. Mellier, *Astron. Astrophys.* **322**, 1 (1997).
 - [32] B. Jain and U. Seljak, *Astrophys. J.* **484**, 560 (1997).
 - [33] P. Schneider, L. van Waerbeke, B. Jain, and G. Kruse, *Mon. Not. R. Astron. Soc.* **296**, 873 (1998).
 - [34] P. J. E. Peebles, *Principles of Physical Cosmology*, Princeton Series in Physics (Princeton University, Princeton, NJ, 1993).
 - [35] A. J. S. Hamilton, A. Matthews, P. Kumar, and E. Lu, *Astrophys. J.* **374**, L1 (1991).
 - [36] J. A. Peacock and S. J. Dodds, *Mon. Not. R. Astron. Soc.* **280**, L19 (1996).
 - [37] A. Cooray and R. Sheth, *Phys. Rep.* **372**, 1 (2002).
 - [38] P. J. Steinhardt, L. Wang, and I. Zlatev, *Phys. Rev. D* **59**, 123504 (1999).

- [39] P. Brax and J. Martin, *Phys. Rev. D* **61**, 103502 (2000).
- [40] P.J.E. Peebles and B. Ratra, *Astrophys. J.* **325**, L17 (1988).
- [41] Y. Wang and P.M. Garnavich, *Astrophys. J.* **552**, 445 (2001).
- [42] U. Alam, V. Sahni, T.D. Saini, and A.A. Starobinsky, *Mon. Not. R. Astron. Soc.* **344**, 1057 (2003).
- [43] D. Huterer and M.S. Turner, *Phys. Rev. D* **60**, 81301 (1999).
- [44] J. Weller and A. Albrecht, *Phys. Rev. Lett.* **86**, 1939 (2001).
- [45] J. Weller and A. Albrecht, *Phys. Rev. D* **65**, 103512 (2002).
- [46] B.F. Gerke and G. Efstathiou, *Mon. Not. R. Astron. Soc.* **335**, 33 (2002).
- [47] T. Padmanabhan and T.R. Choudhury, *Mon. Not. R. Astron. Soc.* **344**, 823 (2003).
- [48] P.S. Corasaniti and E.J. Copeland, *Phys. Rev. D* **67**, 063521 (2003).
- [49] D. Huterer and G. Starkman, *Phys. Rev. Lett.* **90**, 031301 (2003).
- [50] E.V. Linder, *Phys. Rev. Lett.* **90**, 91301 (2003).
- [51] G. Efstathiou, *Mon. Not. R. Astron. Soc.* **310**, 842 (1999).
- [52] L. Van Waerbeke, Y. Mellier, R. Pelló, U.-L. Pen, H. J. McCracken, and B. Jain, *Astron. Astrophys.* **393**, 369 (2002).
- [53] P. Schneider, L. van Waerbeke, M. Kilbinger, and Y. Mellier, *Astron. Astrophys.* **396**, 1 (2002).
- [54] J.M. Bardeen, J.R. Bond, N. Kaiser, and A.S. Szalay, *Astrophys. J.* **304**, 15 (1986).
- [55] D.N. Spergel, L. Verde, H.V. Peiris, E. Komatsu, M.R.olta, C.L. Bennett, M. Halpern, G. Hinshaw, N. Jarosik, A. Kogut *et al.*, *Astrophys. J. Suppl. Ser.* **148**, 175 (2003).
- [56] I. Tereno, O. Dore, L. van Waerbeke, and Y. Mellier, *astro-ph/0404317*.
- [57] A. Refregier, R. Massey, J. Rhodes, R. Ellis, J. Albert, D. Bacon, G. Bernstein, T. McKay, and S. Perlmutter, *Astron. J.* **127**, 3102 (2004).
- [58] J.A. Frieman, D. Huterer, E.V. Linder, and M.S. Turner, *Phys. Rev. D* **67**, 83505 (2003).
- [59] U. Pen, T. Zhang, L. van Waerbeke, Y. Mellier, P. Zhang, and J. Dubinski, *Astrophys. J.* **592**, 664 (2003).
- [60] F. Bernardeau, L. van Waerbeke, and Y. Mellier, *Astron. Astrophys.* **397**, 405 (2003).
- [61] F. Bernardeau, Y. Mellier, and L. van Waerbeke, *Astron. Astrophys.* **389**, L28 (2002).
- [62] L. van Waerbeke, F. Bernardeau, and Y. Mellier, *Astron. Astrophys.* **342**, 15 (1999).
- [63] L. Hui, *Astrophys. J.* **519**, L9 (1999).
- [64] R.E. Smith, J.A. Peacock, A. Jenkins, S.D.M. White, C.S. Frenk, F.R. Pearce, P.A. Thomas, G. Efstathiou, H.M.P. Couchmann, and T.V. Consortium, *Mon. Not. R. Astron. Soc.* **341**, 1311 (2003).
- [65] H. Hoekstra, *Mon. Not. R. Astron. Soc.* **347**, 1337 (2004).